Applied Surface Science 330 (2015) 405–410

Contents lists available at ScienceDirect

Applied Surface Science

journal homepage: www.elsevier.com/locate/apsusc

Amorphous transparent conducting oxides in context: Work function survey, trends, and facile modification

T.C. Yeh[a,b], Q. Zhu[a], D.B. Buchholz[a], A.B. Martinson[b], R.P.H. Chang[a], T.O. Mason[a,*]

[a] Department of Materials Science and Engineering, Northwestern University, Evanston, IL, United States
[b] Material Sciences Division, Argonne National Laboratory, Lemont, IL, United States

ARTICLE INFO

Article history:
Received 10 October 2014
Accepted 3 January 2015
Available online 10 January 2015

Keywords:
Work function
Transparent conducting oxides
Amorphous
TCO
Kelvin probe

ABSTRACT

The work functions of various amorphous and crystalline transparent conducting oxides (TCOs) were measured using Kelvin probe. The films, made by pulsed laser deposition, exhibited varying work functions dependent on the composition and deposition parameters. Tin oxide showed the largest work functions of the oxides measured, while zinc oxide showed the lowest. Binary and ternary combinations of the basis TCOs showed intermediate work functions dependent on the endpoint components. Amorphous TCOs, important in OPV and other technological applications, exhibited similar work functions to their crystalline counterparts. UV/ozone treatment of TCOs temporarily increased the work function, consistent with proposed defect mechanisms associated with near-surface changes in carrier content and Fermi level. Finally, a method for facile adjustment of the work function of commercial TCOs by atomic layer deposition (ALD) capping layers was presented, illustrated by the growth of zinc oxide layers on commercial crystalline ITO films.

1. Introduction

Transparent conducting oxides (TCOs) are an important class of materials used in flat-panel displays, photovoltaics, light-emitting diodes, and electrochromic windows. In these optoelectronic devices, they serve as the transparent electrode, possessing both high electrical conductivity and optical transparency in thin film form. Typically, TCOs are wide-bandgap ($E_g > 3$ eV) semiconductors that are degenerately doped with electron concentrations of between 10^{20} and 10^{21} cm^{-3} and have conductivities greater than 10^3 S/cm [1]. The most common TCO for active devices is currently tin-doped indium oxide, or indium-tin oxide (ITO), but fluorine-doped tin oxide (FTO) has long been employed as a passive TCO in low-emissivity window coatings owing to its high reflectivity in the infrared spectral range. By area, FTO coatings account for more than 4000 km^2 of structural glass per year worldwide [2].

Recently, rising interest in flexible electronics has created the need for TCOs with additional properties. Traditional crystalline TCOs can suffer from film fracture, delamination, and residual film stresses that adversely affect the optoelectronic properties when deposited on flexible substrates [3]. Grain boundaries and multiple grain orientations in polycrystalline films have also been known to decrease carrier mobility by serving as electron scattering centers [2,4]. Amorphous films, however, are comprised of the same materials as crystalline ones, but do not suffer from the issues listed above; they are more mechanically robust, have smoother surfaces, are more easily etched, and require lower deposition/processing temperatures than crystalline films [5]. Unlike covalent semiconductors (e.g. silicon) which rely on aligned sp^3 orbitals for conduction, metal oxide conduction is a consequence of spherically symmetric cation ns orbitals with $(n-1)d^{10}ns^0$ ($ns \geq 4$) electronic configurations, creating overlapping conduction paths that are insensitive to the distorted bond angles found in amorphous materials [6,7]. Therefore, the Hall mobility of these amorphous post-transition metal oxides is similar to that of their crystalline counterparts, whereas a-Si:H has an electron mobility two to three orders of magnitude less than that of single-crystal silicon [7]. The end result is that amorphous metal oxide films have many physical and processing advantages over polycrystalline ones without sacrificing optical/electronic performance.

In the rapidly growing field of organic light-emitting diodes (OLEDs) and organic photovoltaics (OPVs), the band alignment between the TCO and the active layers becomes an added requirement to high transparency and conductivity [8]. Of particular importance is the work function (Φ), defined as the energy required to remove an electron from the Fermi level to the vacuum level [9]. Early OPV studies have shown that the open circuit voltage, V_{OC}, depends highly on the work function difference between the

* Corresponding author. Tel.: +1 847 491 2777.
E-mail address: t-mason@northwestern.edu (T.O. Mason).

http://dx.doi.org/10.1016/j.apsusc.2015.01.026
0169-4332/

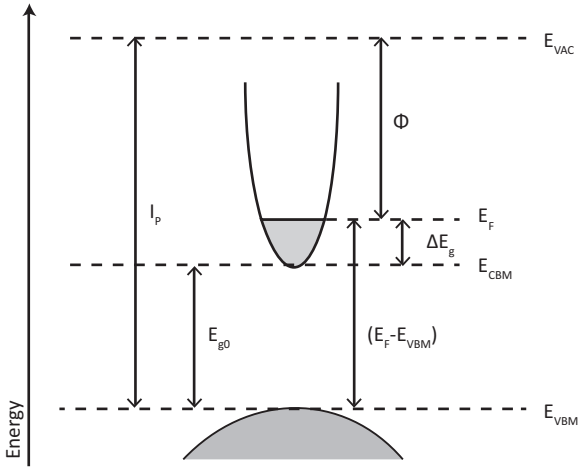

Fig. 1. Schematic TCO band structure and energy levels/differences.

two electrodes, consistent with the metal–insulator–metal model used in thin film solar-cells [10]. Later studies, however, show that V_{OC} depends on the energy level offset between the highest occupied molecular orbital (HOMO) of the donor and the lowest unoccupied molecular orbital (LUMO) of the acceptor [11,12]. Regardless of which model is correct, the appropriate work function alignment is needed to ensure ohmic contact between the electrode and active layers. In order to minimize the barrier for hole injection in normal OPVs, the transparent anode must have a large work function that matches well with the HOMO level of the donor layer (typically >∼5 eV) [13,14]. In inverted OPVs, the transparent cathode requires the contrary: a small work function to match the LUMO of the acceptor or electron transport layer [14]. Other requirements include the traditional high mobility and carrier concentration when processed using a non-vacuum, low-temperature-based deposition approach, as well as protecting the OPV from atmosphere [15].

While ITO is currently the industry standard for transparent electrodes, there are several factors that mitigate against its continued dominance in device applications. First, the relative scarcity and price volatility of indium predicates the need for cheaper and more earth-abundant materials. As flat panel displays become ubiquitous and the demand for TCOs grows in other applications, manufacturers look for lower-cost and price-stable materials. Second, current OPV technology utilizes the hole transport layer PEDOT:PSS, a low-pH organic that has been known to etch ITO, leading to growing interest in other materials that are more chemically robust, such as SnO_2 [16]. Finally, as mentioned above, the work function of the TCO in OPVs should be in excess of 5 eV to match the HOMO level of the organic donor semiconductor to maximize open circuit potential and obviate losses associated with non-ohmic contacts; crystalline ITO (c-ITO) typically has a work function of only 4.7 eV [17]. This last point serves as the motivation for this study: several reviews currently exist for the field of crystalline TCO work functions [2], but less is published on amorphous oxides since they were first presented by the Hosono group more than 10 years ago [7]. This work, therefore, reports for the first time the work functions of several amorphous transparent oxides in order to supplement the existing literature.

2. Theory

A simplified band structure for a degenerately doped n-type semiconductor is shown in Fig. 1. For TCOs, the fundamental band gap (E_{g0}), framed by the valence band maximum (E_{VBM}) and conduction band minimum (E_{CBM}), should be greater than ∼3 eV in order to be transparent to visible light. The shift of the Fermi energy, E_F, from the E_{CBM} into the conduction band by degenerate n-type doping is known as the Burstein-Moss shift, ΔE_g. Depending on the dispersion of the conduction band, degenerate doping can result in as much as 0.5 eV or greater increase in the effective band gap ($E_g + \Delta E_g$) [8]. Finally, the ionization potential, I_P, is the energy required to remove an electron from the valence band maximum to the vacuum level.

As defined previously, the work function (Φ) is the energy required to remove an electron from the Fermi energy to the vacuum level ($E_{VAC} - E_F$). It can also be thought of as the ionization potential minus the Fermi level position ($\Phi = I_P - (E_F - E_{VBM})$). It must be stressed that the work function is not a material constant – it is a surface property that can be changed in one of two ways: (1) by shifting the Fermi level position (via doping) with a constant ionization potential or (2) by changing the ionization potential (via changes in the surface dipoles) with a fixed Fermi energy. There is evidence that the work function in crystalline TCOs can be modified by surface chemical treatment or altering the surface terminations, but so far such work has not been carried out in amorphous TCOs [17].

The work function of a material can be measured using several different methods, including ultraviolet photoelectron spectroscopy (UPS), photoelectron spectroscopy in air (PESA), and Kelvin probe (KP). Because the work function of a material can be extremely sensitive of the surrounding environment (e.g. gases, adsorbed species, humidity, etc.), the most commonly cited method, UPS, occurs under ultra-high vacuum. By isolating the material from the environment, UPS is able to determine an "intrinsic" work function by measuring the kinetic energies (E_{KE}) of photoelectrons excited by incident ultraviolet light ($h\nu$). The binding energy of the sample, calculated from the energy of the incident light, kinetic energy, and the work function of the detector is plotted versus intensity. The work function of the sample is found by taking the difference between the excitation energy and the secondary electron cutoff (the energy after which no secondary electrons are being excited).

The Kelvin probe, unlike UPS, does not require ultrahigh vacuum conditions to measure work function. Therefore, it offers a distinct advantage over UPS of being able to quickly screen the work function of many samples under ambient conditions. Additionally, because most devices (including OPVs) are typically processed in under ambient atmosphere conditions, the KP provides a more relevant description of the work function for industrial applications. The KP also has higher resolution (5–20 meV vs. 100 meV in UPS), which is useful for discerning small changes in sample work function.

The Kelvin probe (KP) is a non-contact technique employing a vibrating capacitor to measure the work function difference between a flat probe and the surface of a specimen of interest. When brought into close proximity of the surface, the vacuum levels are aligned, but each material (probe, specimen under study) has a different Fermi level and therefore different work functions (Fig. 2a). By connecting the two materials externally, the flow of charge equalizes the Fermi energies, but generates an electrostatic potential between the tip and sample, called the contact potential difference or V_{CPD} (Fig. 2b). In this equilibrated state, the potential field equals the work function difference between the materials. By applying a counter potential ($V_{applied}$) until the "zero point" is reached (in Fig. 2c), V_{CPD} can be determined. Because the work function of the tip is known (by calibrating to a known standard, gold in the present work), the work function of the sample can be derived.

Before presenting the work function of TCOs (measured by KP in this work), it is useful to compare and contrast the Kelvin probe method with UPS to determine the presence of any systematic differences. For example, the Kelvin probe measures the average work

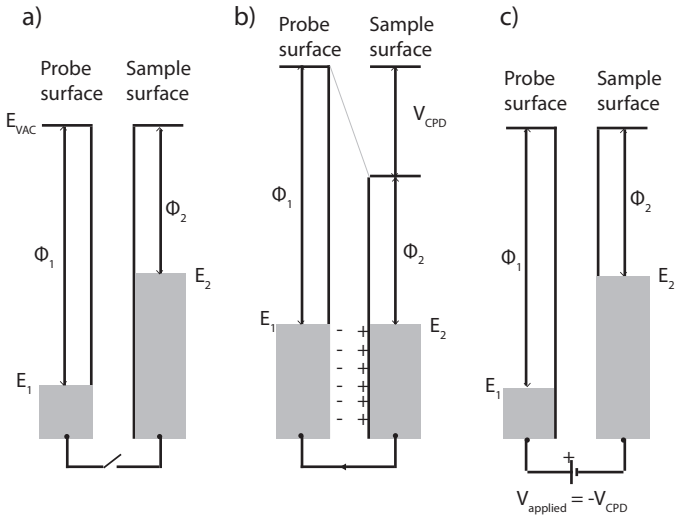

Fig. 2. Energy alignment in Kelvin probe measurements in (a) floating, (b) short-circuit, and (c) voltage-nulling situations.

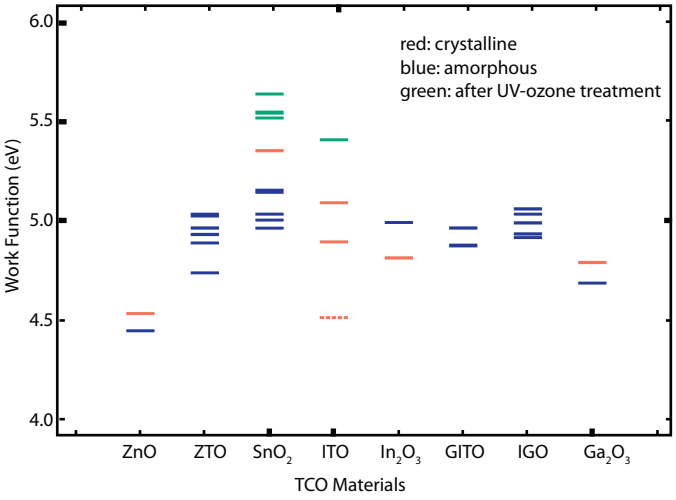

Fig. 3. Work functions by Kelvin probe of amorphous TCOs. The dotted red line indicates a ZnO capping layer on crystalline ITO. (For interpretation of the references to color in this figure legend, the reader is referred to the web version of the article.)

Table 1
Deposition parameters.

Film	Crystalline basis oxides	a-SnO_2, a-ZTO, a-GITO	a-In_2O_3, a-Ga_2O_3, a-IGO	a-ZnO
Temperature	600 °C	25 °C	−25 °C	−100 °C

function under the probe tip, while UPS measures the smallest work function patch on the surface, even if it is only a small fraction of the surface area [18]. Therefore in general, KP measurements of work function tend to be larger than measurements by UPS. In a-ZITO, comparable work functions have been measured by KP and PESA [19–21], but deviate from values reported by UPS [18]. Kim et al. speculates that the irradiation by energetic UV photons in UPS may desorb molecular or atomic species from the surface, the effects of which may be quite large given the sensitivity of the work function to surface dipoles.

3. Experimental details

Amorphous oxide thin-films were grown by pulsed-laser deposition (PLD) from dense, hot-pressed indium oxide, zinc oxide, tin oxide, and gallium oxide targets (25 mm diameter) using a 248 nm KrF excimer laser (25 ns pulse duration at 2 Hz) onto glass or fused silica substrates [4]. The 200 mJ/pulse beam was focused onto a 1 mm × 2 mm spot size, and the target rotated about its axis at 5 rpm to prevent localized heating. Target-substrate separation was fixed at 10 cm. For multi-component films, a computer-controlled shuttle was used to alternate ablation between appropriate basis-oxide targets. Typically, less than one monolayer of material was deposited per cycle to help ensure film composition uniformity; the desired film composition was obtained by adjusting the ratio of the pulses for each metal oxide cycle. A resistively-heated substrate holder was used to grow films above room temperature, whereas a liquid nitrogen-cooled holder was used to grow films at lower temperatures. A table of deposition temperatures for the various oxides is shown in Table 1.

Grazing incidence X-ray diffraction measurements confirmed the lack of long-range order in amorphous films. Amorphous and crystalline samples of the basis oxides (In_2O_3, SnO_2, Ga_2O_3, and ZnO) were grown and measured by KP without surface treatment. Binary and ternary amorphous oxides (a-ZTO, a-IGO, and a-GITO) were also examined. Crystalline ITO, purchased commercially, was used for comparison. The c-ITO and a-SnO_2 were further treated with UV/ozone for 10 min and measured for comparison.

Sheet resistance (R_s: Ω/□), carrier type, area carrier-concentration (n_a: 1 cm^{-2}), and carrier mobility (μ: $cm^2/V\,s$) were measured with an Ecopia 3000 Hall measurement system on samples in the van der Pauw geometry. Carrier density (n_v: 1 cm^{-3}) and resistivity (ρ: Ω cm) were calculated by dividing the area carrier-concentration and sheet resistance, respectively, by the film thickness. Film thickness (d: nm) was measured using a spectral reflectometer (Filmetrics F20).

Kelvin probe measurements were carried out using a non-scanning ambient Kelvin probe system (KP Technology, Inc., Wick, Scotland). The work function of the 2-mm gold-coated probe tip was calibrated using a gold standard (Φ = 5.1 eV) before and after measurements to ascertain the stability of the apparatus and establish a baseline for experimental error. Although gold is considered to be inert, factors like humidity can still affect the work function of the probe tip; therefore, a dehumidifier was used to maintain the relative humidity in the room below 45 percent. The film cleaning process prior to KP measurements involved rinsing in ethanol, acetone, hexane, and deionized water, followed by a nitrogen gun for drying. Multiple measurements (typically three) were made on each sample at different locations to ensure reproducibility. Each film was mounted with a small strip of aluminum or copper tape for electrical grounding.

4. Results and discussion

4.1. Kelvin probe measurements of a-TCOs

The work functions of a-TCOs are summarized in Fig. 3. Detailed information regarding deposition pO_2 and post-deposition surface treatments are available in Table 3. Out of the crystalline undoped basis oxides (i.e. In_2O_3, SnO_2, Ga_2O_3, ZnO), c-SnO_2 has the largest work function, ~5.3 eV, while ZnO has the smallest, ~4.5 eV. In_2O_3 and Ga_2O_3 had work functions in between that of ZnO and SnO_2. The commercially purchased c-ITO has a reported work function of 4.7 eV by UPS, but was measured between 4.9 and 5.1 eV by KP in this work.

For amorphous phases, the work functions are generally comparable to that of the corresponding crystalline phase, or even slightly larger in the case of In_2O_3 (4.99 eV for a-In_2O_3 vs. 4.81 eV for c-In_2O_3). For a-SnO_2 samples deposited under different oxygen

Table 2
Ambient KP work functions.

Material	Phase	Deposition pO_2 (mTorr)	Surface treatment	WF (eV)	Carrier conc.	Mobility	Conductivity
ITO	c	–	–	4.89	6.16E20	42.6	4.21E3
ITO**	c	–	UV/ozone	5.40	–	–	–
ZnO-ITO	c	(400 cy. ALD)	–	4.50	1.85E21	40.1	4.31E3
ZnO*	c	7.5	–	4.53	–	–	<0.1
ZnO*	a	7.5	–	4.44	–	–	<0.1
Ga_2O_3*	c	7.5	–	4.79	–	–	<0.1
Ga_2O_3*	a	7.5	–	4.68	–	–	<0.1
SnO_2	c	7.5	–	5.35	6.10E18	2.3	0.46
SnO_2	a	8	–	4.96	2.16E19	5.59	2.19E1
SnO_2	a	10	–	5.00	8.53E19	23.3	4.09E2
SnO_2	a	12	–	5.15	1.44E20	20.0	4.61E2
SnO_2	a	14	–	5.03	1.34E20	22.4	4.29E2
SnO_2	a	16	–	5.14	1.10E20	23.2	4.07E2
SnO_2**	a	10	UV/ozone	5.54			
SnO_2**	a	12	UV/ozone	5.51			
SnO_2**	a	14	UV/ozone	5.54			
SnO_2**	a	16	UV/ozone	5.63			
In_2O_3	c	7.5	–	4.81	5.1E18	60.4	49
In_2O_3	a	7.5	–	4.99	2.7E20	53.5	2290
ZTO70	a	10	–	4.93	2.1E19	11.6	38.9
ZTO90	a	10	–	5.02	1.0E20	18.6	297
ZTO70	a	7.5	–	4.73	2.3E19	12.0	43.0
ZTO90	a	7.5	–	4.96	1.1E20	21.4	375
IGO2.5	a	7.5	–	5.03	2.0E20	51	1620
IGO5	a	7.5	–	4.99	2.5E20	36	1470
IGO10	a	7.5	–	4.91	1.9E20	32	990
IGO12.5	a	7.5	–	4.93	2.1E20	30	1020
IGO15	a	7.5	–	4.93	1.6E20	37	970
IGO20	a	7.5	–	5.06	9.6E19	36	550
GITO60	a	7.5	–	4.96	7.6E19	28.2	344
GITO80	a	7.5	–	4.87	2.2E20	33.5	1170

* These films were too resistive to be measured.
** These films were not time-stable.

partial pressures, work functions range between 4.96 and 5.15 eV, but show no clear trend with deposition pressure. Differences may arise from different SnO_2 surface terminations; for example it was shown previously that Sn^{2+} can occur at low deposition pO_2 values [22]. However, the variation is not significant given the experimental error. While the KP has excellent resolution (5–30 meV), the stability of the probe may have affected the accuracy of the measured work functions; the contact potential difference was frequently observed to drift as much as 50 meV over the course of 2 h. As such, 50 meV is considered the error range for the work functions measured in this study.

The work function of amorphous zinc-doped tin oxide (a-ZTO) varied between 4.7 and 5.0 eV, smaller than a-SnO_2, but larger than a-ZnO, indicative that the work function of a binary oxide may be some "average" of its respective component oxides. It should be noted that these KP work functions were also consistently larger than those measured in UPS (4.32–4.62 eV). The ionization potential measured by UPS for those samples ranged from 7.65 to 7.8 eV, possibly indicating that the changes in work function are due to changes in surface states. In device applications, the smaller work function of ZTO films may make them more suitable for inverted organic solar cell applications.

Work functions of amorphous binary and ternary cation TCOs are also shown in Fig. 3 and Table 2 (a-ZTO, a-IGO, a-GITO). Amorphous IGO and GITO have work functions ranging between 4.9 and 5.1 eV, with carrier concentrations on the order of 10^{20} cm^{-3}. These values are larger than the results obtained by Goncalves et al., where a monotonic decrease of work function from 4.84 to 4.53 eV was observed for a-IGO films, corresponding to carrier concentration increases from 10^{13} to 10^{19} cm^{-3} [23]. While the latter trend can be traced to a shift in Fermi level due to doping, the same explanation cannot be applied to the present data. The determination of whether the work function changes owing to Fermi level shifts or surface dipole changes has yet to be investigated for the a-IGO in this work. Nevertheless, the work functions of a-IGO and a-GITO are slightly larger than that of c-ITO, and thus may be promising for organic-based devices in traditional polarity.

4.2. UV/ozone treatment

The effect of UV/ozone treatment was investigated in c-ITO and a-SnO_2 films. A consistent increase in work function (0.4–0.5 eV) was observed after 10 min of UV/ozone treatment. Proffit et al. observed similar increases in work function and ionization potential with ozone treatment or high temperature annealing in dry air (2 h at 450 °C) [19]. However, after exposure to air, the gains in work function would disappear over a period of hours or days. A possible explanation for this behavior is that ozone, a strong oxidant, oxidizes the film near the surface, filling oxygen vacancies. Because these films were not time-stable after ozone treatment, efforts to characterize the carrier concentration and Hall mobility proved inconclusive. However, the following argument is presented as a likely explanation for the measured changes in work function. Conduction in c-ITO is well-known to be associated with the concentration of oxygen vacancies, but the mechanisms present in amorphous oxides are less clear. Lee and Paine suggest that in a-IZO, carrier density is dependent on "oxygen vacancy-like" donor defects [24]. While the defect mechanisms have yet to be elucidated for amorphous tin oxide, it may be safe to assume that "oxygen vacancy-like" defects are similarly the dominant species in conduction. With fewer defect sites, the free carrier concentration of the film decreases, manifesting as a decrease in the Fermi energy, and therefore an increase in the work function. After ozone treatment is completed, the film slowly re-equilibrates with atmospheric oxygen levels, releasing oxygen and regenerating oxygen vacancies, reversing the effects of ozone treatment.

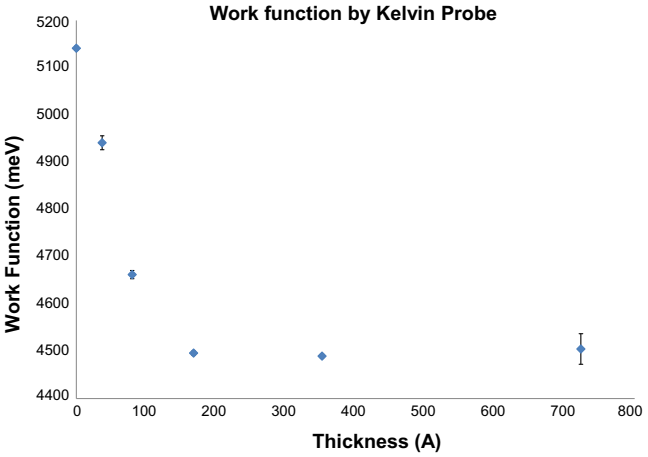

Fig. 4. Work functions by Kelvin probe of crystalline ITO with zinc oxide capping layers of varying thicknesses.

Table 3
In-plane resistance as a function of the number of ZnO capping layers.

ZnO cycles	0	25	50	100	200	400
Thickness (A)	0	37	80	168	352	723
Resistance (ohm)	11.9	11.2	12.2	11.8	11.9	11.6

4.3. Modification of work function by atomic layer deposition

Given the fact that the work function of multi-cation TCOs seem to be some linear combination of its component oxides, an effort was made to determine whether the work function of a particular TCO could be modified by depositing a layer of another TCO with a different work function on the surface of the substrate TCO. In particular, atomic layer deposition (ALD) was used to deposit thin layers of zinc oxide on top of commercial ITO to test the overall effect on work function. ALD operates by using gaseous precursors to deposit films in a controlled layer-by-layer fashion via chemical half reactions. If the work function is indeed adjustable by only the surface, it could be valuable in device applications while maintaining the bulk transport properties of the film. In this study we show preliminary results where zinc oxide, grown by ALD using diethylzinc and water, modulates the work function of the ITO substrate. Between 5 and 400 cycles of zinc oxide were deposited at 140 °C using a Savannah ALD reactor (Cambridge Nanotech, Waltham, MA). Results are shown in Fig. 4.

Because the work function of zinc oxide is smaller than the work function of ITO, layers of ZnO might be expected to decrease the overall work function of ZnO on ITO from that of uncapped ITO. As shown in Fig. 4, this is indeed the case. The work function, measured by Kelvin probe, is seen to decrease progressively as more layers of ZnO are deposited. After 200 cycles of ZnO (170 Å), however, the work function saturates at a level consistent with that of zinc oxide, which at that point completely masks the underlying ITO. It should be noted, however, that the in-plane resistance of the films remained unchanged after the addition of the zinc oxide capping layers, as summarized in Table 3. Further investigation into the underlying physical mechanisms (band bending, surface doping, etc.) is necessary to fully understand the change in work function; nevertheless, this finding may have important implications for device manufacturing where the work function of TCOs can be tailored to particular specifications.

5. Conclusions

In this study, the work function of basis, binary, and certain ternary cation transparent conducting oxides were measured using ambient Kelvin probe. In general, amorphous TCOs had work functions similar to their crystalline counterparts, and confirmed the general trend of tin oxide having relatively larger work functions than those of both gallium oxide and zinc oxide (the smallest of the measured TCOs). Binary and ternary cation TCOs exhibited work functions that were intermediate to those of their endpoint components, suggesting that work functions can be tailored by composition. This point was demonstrated by using ALD to deposit ZnO layers on crystalline ITO films, decreasing the work function but maintaining bulk properties. Finally, UV/ozone treatment of c-ITO and a-SnO_2 indicated that the work function may be temporarily altered by changing the near-surface oxygen vacancy concentration of the bulk film.

Acknowledgements

This work was supported as part of the Argonne-Northwestern Solar Energy Research Center (ANSER), an energy Frontier Research Center funded by the U.S. Department of Energy Office of Science, Basic Energy Sciences under award #DE-SC0001059.

References

[1] M.P. Taylor, D.W. Readey, M.F.A.M. van Hest, C.W. Teplin, J.L. Alleman, M.S. Dabney, L.M. Gedvilas, B.M. Keyes, B. To, J.D. Perkins, D.S. Ginley, The remarkable thermal stability of amorphous In–Zn–O transparent conductors, Adv. Funct. Mater. 18 (20) (2008) 3169–3178.
[2] K. Ellmer, Past achievements and future challenges in the development of optically transparent electrodes, Nat. Photonics 6 (12) (2012) 809–817.
[3] M. Kumar, A.K. Sigdel, T. Gennett, J.J. Berry, J.D. Perkins, D.S. Ginley, C.E. Packard, Optimizing amorphous indium zinc oxide film growth for low residual stress and high electrical conductivity, Appl. Surf. Sci. 283 (2013) 65–73.
[4] Q. Zhu, Q. Ma, D.B. Buchholz, R.P.H. Chang, M.J. Bedzyk, T.O. Mason, Structural anisotropy in amorphous SnO_2 film probed by X-ray absorption spectroscopy, Appl. Phys. Lett. 103 (3) (2013) 031913.
[5] C. Lee, W. Lee, H. Kim, H.W. Kim, Influence of annealing atmosphere on the structure, resistivity and transmittance of InZnO thin films, Ceram. Int. 34 (4) (2008) 1089–1092.
[6] R. Martins, P. Barquinha, A. Pimentel, L. Pereira, E. Fortunato, Transport in high mobility amorphous wide band gap indium zinc oxide films, Phys. Status Solidi 202 (9) (2005) R95–R97.
[7] K. Nomura, H. Ohta, A. Takagi, T. Kamiya, M. Hirano, H. Hosono, Room-temperature fabrication of transparent flexible thin-film transistors using amorphous oxide semiconductors, Nature 432 (7016) (2004) 488–492.
[8] A. Klein, C. Körber, A. Wachau, F. Säuberlich, Y. Gassenbauer, S.P. Harvey, D.E. Proffit, T.O. Mason, Transparent conducting oxides for photovoltaics: manipulation of fermi level, work function and energy band alignment, Materials (Basel) 3 (11) (2010) 4892–4914.
[9] H. Ishii, K. Sugiyama, E. Ito, K. Seki, Energy level alignment and interfacial electronic structures at organic/metal and organic/organic interfaces, Adv. Mater. 11 (8) (1999) 605–625.
[10] M.F. Lo, T.W. Ng, T.Z. Liu, V.A.L. Roy, S.L. Lai, M.K. Fung, C.S. Lee, S.T. Lee, Limits of open circuit voltage in organic photovoltaic devices, Appl. Phys. Lett. 96 (11) (2010) 113303.
[11] M.C. Scharber, D. Mühlbacher, M. Koppe, P. Denk, C. Waldauf, A.J. Heeger, C.J. Brabec, Design rules for donors in bulk-heterojunction solar cells—towards 10% energy-conversion efficiency, Adv. Mater. 18 (6) (2006) 789–794.
[12] B. Rand, D. Burk, S. Forrest, Offset energies at organic semiconductor heterojunctions and their influence on the open-circuit voltage of thin-film solar cells, Phys. Rev. B 75 (11) (2007) 115327.
[13] E. Fortunato, A. Pimentel, A. Goncalves, A. Marques, R. Martins, High mobility amorphous/nanocrystalline indium zinc oxide deposited at room temperature, Thin Solid Films 2 (2006) 104–107.
[14] S.B. Darling, F. You, The case for organic photovoltaics, RSC Adv. 3 (2013) 17633–17648.
[15] E. Fortunato, D. Ginley, H. Hosono, D.C. Paine, Transparent conducting oxides for photovoltaics, MRS Bull. 32 (March) (2007) 242–247.
[16] B.P. Singh, R. Kumar, A. Kumar, J. Gaur, S.P. Singh, R.C. Tyagi, Effect of annealing on properties of transparent conducting tin oxide films deposited by thermal evaporation, Indian J. Pure Ap. Phys. 51 (8) (2013) 558–562.
[17] Q. Zhu, Physical Properties and Local Structures of Amorphous Zn–Sn–O and Amorphous In–Ga–O Films, Northwestern University, PhD dissertation, 2013.
[18] J.S. Kim, B. Lägel, E. Moons, N. Johansson, I.D. Baikie, W.R. Salaneck, R.H. Friend, F. Cacialli, Kelvin probe and ultraviolet photoemission measurements of indium tin oxide work function: a comparison, Synth. Met. 111 (2000) 311–314.
[19] D.E. Proffit, S.P. Harvey, A. Klein, R. Schafranek, J.D. Emery, D.B. Buchholz, R.P.H. Chang, M.J. Bedzyk, T.O. Mason, Surface studies of crystalline and amorphous Zn–In–Sn–O transparent conducting oxides, Thin Solid Films 520 (17) (2012) 5633–5639.

[20] G.S. Heo, Y. Matsumoto, I.G. Gim, H.K. Lee, J.W. Park, T.W. Kim, Transparent conducting amorphous Zn–In–Sn–O anode for flexible organic light-emitting diodes, Solid State Commun. 150 (3–4) (2010) 223–226.
[21] C.W. Ow-Yang, H. Yeom, D.C. Paine, Fabrication of transparent conducting amorphous Zn–Sn–In–O thin films by direct current magnetron sputtering, Thin Solid Films 516 (10) (2008) 3105–3111.
[22] M. Alaf, M.O. Guler, D. Gultekin, M. Uysal, A. Alp, H. Akbulut, Effect of oxygen partial pressure on the microstructural and physical properties on nanocrystalline tin oxide films grown by plasma oxidation after thermal deposition from pure Sn targets, Vacuum 83 (2) (2008) 292–301.
[23] G. Gonçalves, P. Barquinha, L. Pereira, N. Franco, E. Alves, R. Martins, E. Fortunato, High mobility a-IGO films produced at room temperature and their application in TFTs, Electrochem. Solid-State Lett. 13 (1) (2010) H20.
[24] S. Lee, D.C. Paine, Identification of the native defect doping mechanism in amorphous indium zinc oxide thin films studied using ultra high pressure oxidation, Appl. Phys. Lett. 102 (5) (2013) 052101.